Electronic Supplementary Material (ESI) for Photochemical & Photobiological Science

Electronic Supporting Information

Photophysical properties of 3-[2-(N-phenylcarbazolyl)benzoxazol-5-yl]alanine derivatives – experimental and theoretical studies

Katarzyna Guzow[a,], Marlena Czerwińska[a], Agnieszka Ceszlak[a], Marta Kozarzewska[a], Mariusz Szabelski[b,c], Cezary Czaplewski[a], Anna Łukaszewicz[b], Aleksander A. Kubicki[b], Wiesław Wiczk[a]*

[a] Faculty of Chemistry, University of Gdańsk, Sobieskiego 18, 80-952 Gdańsk, Poland

[b] Institute of Experimental Physics, Faculty of Mathematics, Physics and Informatics, Univeristy of Gdańsk, Wita Stwosza 57, 80-952 Gdańsk, Poland

[c] Current address (M. Sz.): Department of Physics and Biophysics, University of Warmia and Mazury in Olsztyn, Oczapowskiego 4, 10-719 Olsztyn, Poland

[*] corresponding author: e-mail: kasiag@chem.univ.gda.pl

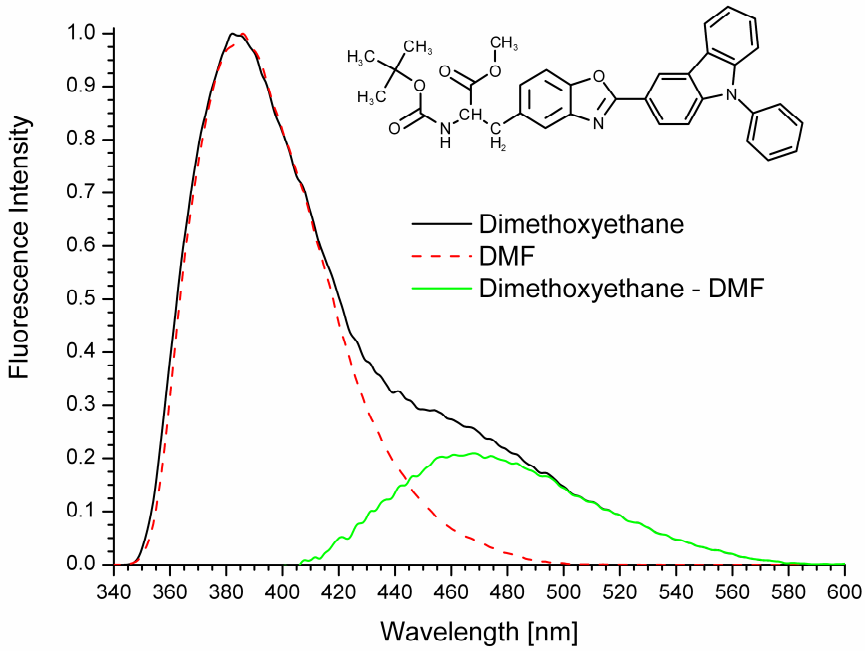

Figure 1S. Fluorescence spectra of **2** in dimethoxyethane and DMF as well as the spectrum of its exciplex formed in dimethoxyethane obtained as a difference between these spectra.

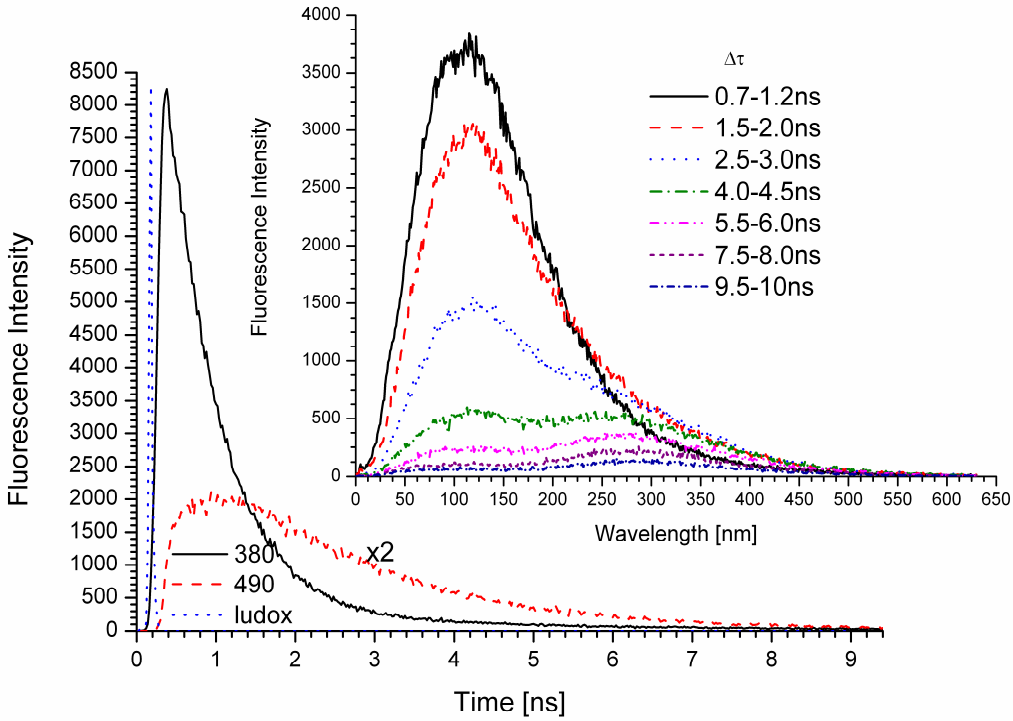

Figure 2S. Fluorescence intensity decay observed at 380 nm and 490 nm as well as time-resolved spectra of **2** in dimethoxyethane.

Table 1S. The values of estimated coefficients (y_0 and a) and their standard errors as well as regression coefficients (r) obtained from the linear fit of photophysical properties ($\tilde{\nu}_{abs}$, $\tilde{\nu}_{fluo}$, $\Delta\tilde{\nu}$, φ_F and τ) of **1** versus E_T^N solvent polarity scale. Np denotes a number of solvents used in the analysis.

Compound **1**					
y		Equation $y=(y_0 \pm a) + (b \pm c)*E_T^N$		r	Np
		$y_0 \pm a$	$b \pm c$		
$\tilde{\nu}_{abs}$ [cm^{-1}]	all solvents	29350±40	-(230±90)	0.2933	22
	aprotic	29370±50	-(260±200)	0.3709	12
	protic	29390±180	-(170±290)	0.1989	10
$\tilde{\nu}_{fluo}$ [cm^{-1}]	all solvents	26140±390	-(5900±840)	0.8440	22
	aprotic	26930±350	-(10920±1290)	0.9366	12
	protic	27560±1050	-(7550±1680)	0.8464	10
$\Delta\tilde{\nu}$ [cm^{-1}]	all solvents	3210±380	5780±830	0.8423	22
	aprotic	2450±340	10660±1260	0.9362	12
	protic	1830±1090	7390±1750	0.8310	10
φ_F	all solvents	0.65±0.06	-(0.12±0.12)	0.3354	22
	aprotic	0.70±0.05	-(0.57±0.20)	0.4652	12
	protic	1.18±0.14	-(0.90±0.22)	0.8156	10
τ [ns]	all solvents	1.83±0.28	5.06±0.60	0.8834	22
	aprotic	1.21±0.13	9.00±0.50	0.9849	12
	protic	0.87±0.94	6.10±1.50	0.8220	10

Table 2S. The values of estimated coefficients (y_0 and a) and their standard errors as well as regression coefficients (r) obtained from the linear fit of photophysical properties ($\tilde{\nu}_{abs}$, $\tilde{\nu}_{fluo}$, $\Delta\tilde{\nu}$, φ_F and τ) of **2** versus E_T^N solvent polarity scale. Np denotes a number of solvents used in the analysis.

Compound **2**					
y		Equation $y=(y_0 \pm a) + (b \pm c)*E_T^N$		r	Np
		$y_0 \pm a$	$b \pm c$		
$\tilde{\nu}_{abs}$ [cm^{-1}]	all solvents	30711±94	-(769±220)	0.5387	32
	aprotic	30643±50	-(274±171)	0.3364	21
	protic	30480±1050	-(558±1660)	0.1179	11
$\tilde{\nu}_{fluo}$ [cm^{-1}]	all solvents	26688±64	-(1682±149)	0.8998	32
	aprotic	26736±57	-(2119±195)	0.9250	21
	protic	27686±319	-(3094±505)	0.9080	11
$\Delta\tilde{\nu}$ [cm^{-1}]	all solvents[a]	4023±101	913±235	0.5784	31
	aprotic	3907±44	1846±149	0.9402	21
	protic	2794±839	2537±1328	0.5560	11
φ_F	all solvents[a]	0.74±0.03	0.41±0.08	0.6705	31
	aprotic	0.72±0.05	0.55±0.20	0.5528	21
	protic	0.93±0.05	0.09±0.07	0.4008	10
τ [ns]	all solvents[b]	2.01±0.08	-(0.65±0.18)	0.5542	30
	aprotic	2.11±0.10	-(1.17±0.39)	0.5803	20
	protic	1.02±0.08	0.97±0.13	0.9339	10

[a] without formamide
[b] without formamide and dimethoxyethane

Table 3S. Estimated from eq. 3 coefficients (y_o. a_{SPP}, b_{SA}, c_{SB}), their standard errors and correlation coefficients (r) for the multiple linear regression analysis of $\tilde{\nu}_{abs}$, $\tilde{\nu}_{fluo}$, $\Delta\tilde{\nu}$, φ_F, τ of **1** as a function of Catalán three-parameter solvent scale.

y	y_0	SPP	SA	SB	r
$\tilde{\nu}_{abs}$ [cm^{-1}]	29438±50 29445±41	-(276±87) -(263±72)	-(2±62)	-(26±101)	0.6448 0.6422
$\tilde{\nu}_{fluo}$ [cm^{-1}]	27340±371	-(4857±651)	-(1359±460)	-(1005±755)	0.9403
$\Delta\tilde{\nu}$ [cm^{-1}]	-(3909±860) -(3782±836)	11537±1232 11087±1080	2148±606 2039±584	-(447±567)	0.9540 0.9524
φ_F	0.82±0.14 0.83±0.13	-(0.54±0.20) -(0.55±0.19)	-(0.02±0.10)	0.35±0.09 0.35±0.09	0.6870 0.6859
τ [ns]	-(4.04±0.51)	9.77±0.74	2.24±0.36	-(0.66±0.34)	0.9771

Table 4S. Estimated from eq. **2** coefficients (y_o, a_{π^*}, b_α, c_β,), their standard errors and correlation coefficients (r) for the multiple linear regression analysis of $\tilde{\nu}_{abs}$, $\tilde{\nu}_{fluo}$, $\Delta\tilde{\nu}$, φ_F, τ of **1** as a function of Kamlet-Taft solvent scale.

y	y_0	π^*	α	β	r
$\tilde{\nu}_{abs}$ [cm^{-1}]	29438±50 29445±41	-(276±87) -(263±72)	-(2±62)	-(26±101)	0.6448 0.6422
$\tilde{\nu}_{fluo}$ [cm^{-1}]	27340±371	-(4857±651)	-(1359±460)	-(1005±755)	0.9403
$\Delta\tilde{\nu}$ [cm^{-1}]	2098±406 2323±370	4580±713 4988±643	1357±503 1754±396	1031±825	0.9252 0.9180
φ_F	0.53±0.05 0.57±0.05	-(0.25±0.10) -(0.24±0.09)	-(0.02±0.07)	0.27±0.11 0.24±0.09	0.6016 0.5981
τ [ns]	1.00±0.31 1.15±0.27	3.87±0.54 4.13±0.48	1.34±0.58 1.64±0.29	0.64±0.62	0.9407 0.9367

Table 5S . Estimated from eq. **3** coefficients (y_o. a_{SPP}, b_{SA}, c_{SB}), their standard errors and correlation coefficients (r) for the multiple linear regression analysis of $\tilde{\nu}_{abs}$, $\tilde{\nu}_{fluo}$, $\Delta\tilde{\nu}$, φ_F, τ of **2** as a function of Catalán three-parameter solvent scale.

y	y_0	SPP	SA	SB	r
$\tilde{\nu}_{abs}$ [cm^{-1}]	31027±287	-(678±426)	-(1002±252)	-(154±200)	0.5218
	30966±269	-(516±363)	-(958±235)		0.5154
$\tilde{\nu}_{fluo}$ [cm^{-1}]	27354±269	-(1361±399)	-(1606±326)	-(142±188)	0.7959
	23087±255	-(1238±343)	-(1536±222)		0.7883
$\Delta\tilde{\nu}$ [cm^{-1}]	3679±340	672±505	596±294	37±234	0.5669
	3665±322	711±434	607±281		0.5664
φ_F	0.40±0.13	0.58±0.20	0.16±0.12	-(0.01±0.09)	0.6553
	0.34±0.12	0.68±0.15			0.6276
τ [ns]	2.86±0.25	-(1.25±0.37)	1.38±0.22	-(2.29±0.18)	0.6962

Table 6S. Estimated from eq. **2** coefficients (y_o, a_{π^*}, b_α, c_β,), their standard errors and correlation coefficients (r) for the multiple linear regression analysis of $\tilde{\nu}_{abs}$, $\tilde{\nu}_{fluo}$, $\Delta\tilde{\nu}$, φ_F, τ of **2** as a function of Kamlet-Taft solvent scale.

y	y_0	π^*	α	β	r
$\tilde{\nu}_{abs}$ [cm^{-1}]	30721±92	-(458±165)	-(579±159)	-(229±216)	0.5135
	30759±85	-(393±154)	-(467±119)		0.4946
$\tilde{\nu}_{fluo}$ [cm^{-1}]	26760±85	-(974±152)	-(780±147)	-(164±199)	0.7990
	26788±78	-(928±140)	-(699±109)		0.7942
$\Delta\tilde{\nu}$ [cm^{-1}]	3962±106	515±189	216±183	60±248	0.6021
	3972±96	531±173	254±134		0.6010
φ_F	0.73±0.04	0.22±0.07	0.14±0.07	0.00±0.10	0.6761
	0.73±0.04	0.22±0.06	0.15±0.05		0.6761
τ [ns]	2.16±0.08	-(0.44±0.14)	-(0.08±0.14)	-(0.26±0.19)	0.7091
	2.17±0.08	-(0.44±0.14)		-(0.34±0.14)	0.7046

Table 7S. Theoretically calculated absorption wavelengths (for f≥0.1) for **1** using def2-TZVP/pbe0 functional.

acetonitrile				cyclohexane			
λ [nm]	f	MO contribution	(%)	λ [nm]	f	MO contribution	(%)
355.5	0.565	HOMO → LUMO	98.0	356.9	0.248	HOMO → LUMO	98.0
308.3	0.07	HOMO → LUMO+1	92.0	307.2	0.075	HOMO → LUMO+1	91.9
290.5	0.483	HOMO-2 → LUMO	93.0	291.0	0.517	HOMO-2 → LUMO	92.5
271.7	0.112	HOMO-3 → LUMO	89.2	271.2	0.112	HOMO-1 → LUMO+1	73.1
		HOMO-2 → LUMO	3.6			HOMO → LUMO+4	20.8
236.4	0.351	HOMO → LUMO+4	39.1	272.0	0.095	HOMO-3 → LUMO	89.5
		HOMO-4 → LUMO	25.4			HOMO-4 → LUMO	3.4
		HOMO-1 → LUMO+1	10.3				
		HOMO-2 → LUMO+2	6.6	237.3	0.364	HOMO → LUMO+4	49.6
281.2	0.260	HOMO-1 → LUMO+6	4.3			HOMO-4→ LUMO	12.9
		HOMO → LUMO+7	4.0			HOMO-1 → LUMO+1	10.6
		HOMO-1 → LUMO+3	2.4			HOMO-1 → LUMO+6	6.0
						HOMO → LUMO+7	4.7
225.3	0.198	HOMO-4→ LUMO+1	55.8			HOMO-2 → LUMO+2	4.7
		HOMO-1 → LUMO+3	8.7			HOMO-1 → LUMO+3	3.4
		HOMO-1 → LUMO	8.4				
		HOMO-1 → LUMO+6	8.3	225.7	0.228	HOMO-4 → LUMO+1	49.8
		HOMO → LUMO+4	6.7			HOMO-1 → LUMO+3	11.4
		HOMO-2 → LUMO+2	3.0			HOMO-1 → LUMO	8.6
						HOMO → LUMO+4	8.5
222.0	0.149	HOMO-6 → LUMO	30.0			HOMO-1 → LUMO+6	7.5
		HOMO-2 → LUMO+3	24.5			HOMO-5 → LUMO	4.3
		HOMO-1 → LUMO+4	18.8				
		HOMO → LUMO+3	8.2	222.3	0.163	HOMO-6 → LUMO	53.1
		HOMO-3 → LUMO+1	3.2			HOMO-2 → LUMO+3	22.9
		HOMO → LUMO+5	2.7			HOMO-1 → LUMO+4	8.8
		HOMO-2 → LUMO+1	2.6			HOMO → LUMO+3	5.7
		HOMO-6 → LUMO+1	0.9				

Table 8S. Theoretically calculated absorption wavelengths (for f≥0.1) for **2** using def2-TZVP/pbe0 functional.

acetonitrile				cyclohexane			
λ [nm]	f	MO contribution	(%)	λ [nm]	f	MO contribution	(%)
326.2	0.580	HOMO → LUMO	85.4	323.5	0.490	HOMO → LUMO	78.6
		HOMO → LUMO+1	8.2			HOMO → LUMO+1	13.7
315.9	0.210	HOMO→ LUMO+1	71.5	314.3	0.350	HOMO+1 → LUMO+1	67.5
		HOMO-1→ LUMO	14.8			HOMO → LUMO	15.2
		HOMO →LUMO	8.5			HOMO-1→ LUMO	12.3
288.5	0.565	HOMO-2 → LUMO	71.5	286.8	0.512	HOMO-1 → LUMO	69.8
		HOMO-2 → LUMO+1	10.5			HOMO-1 → LUMO+1	13.1
		HOMO → LUMO+1	9.0	271.2	0.112	HOMO → LUMO+1	6.3
						HOMO→ LUMO	2.6
261.6	0.112	HOMO-1 → LUMO+2	31.5				
		HOMO-3 → LUMO+6	22.8	262.1	0.225	HOMO-1 → LUMO+1	33.7
		HOMO → LUMO+7	11.1			HOMO-3 → LUMO	25.9
		HOMO-2 → LUMO+3	7.1			HOMO-2 → LUMO	15.5
		HOMO→ LUMO+1	4.8	237.3	0.364	HOMO → LUMO+5	4.9
		HOMO-1 → LUMO+3	2.8			HOMO → LUMO+2	4.0
		HOMO → LUMO	2.2			HOMO-1 → LUMO	3.2
		HOMO-1 → LUMO+6	2.1			HOMO → LUMO	2.4

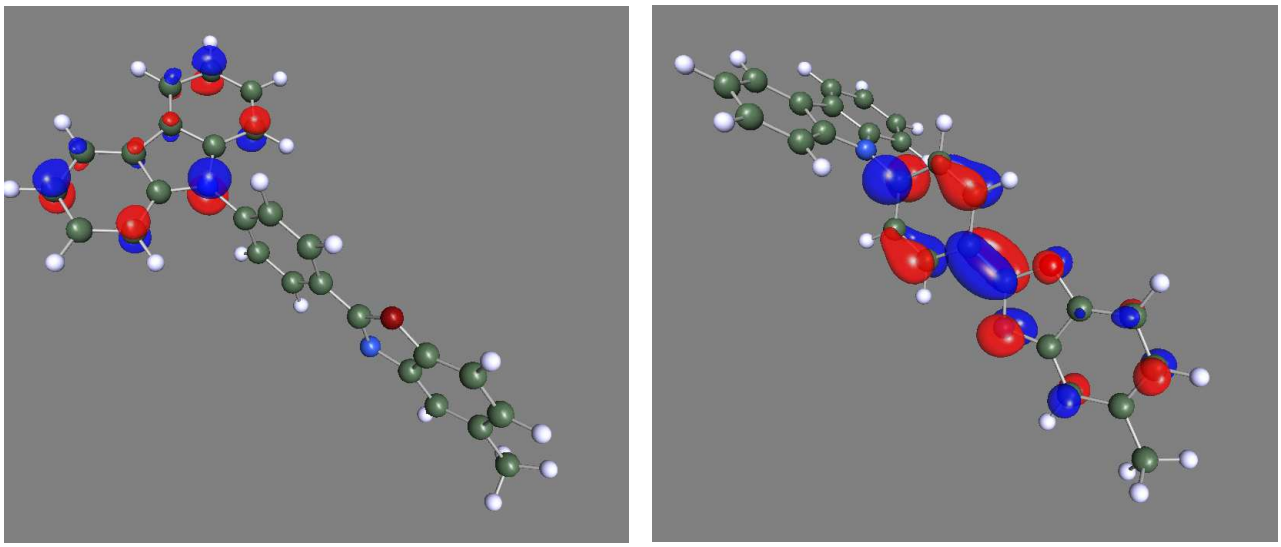

Figure 3S. HOMO and LUMO orbitals of **1**.

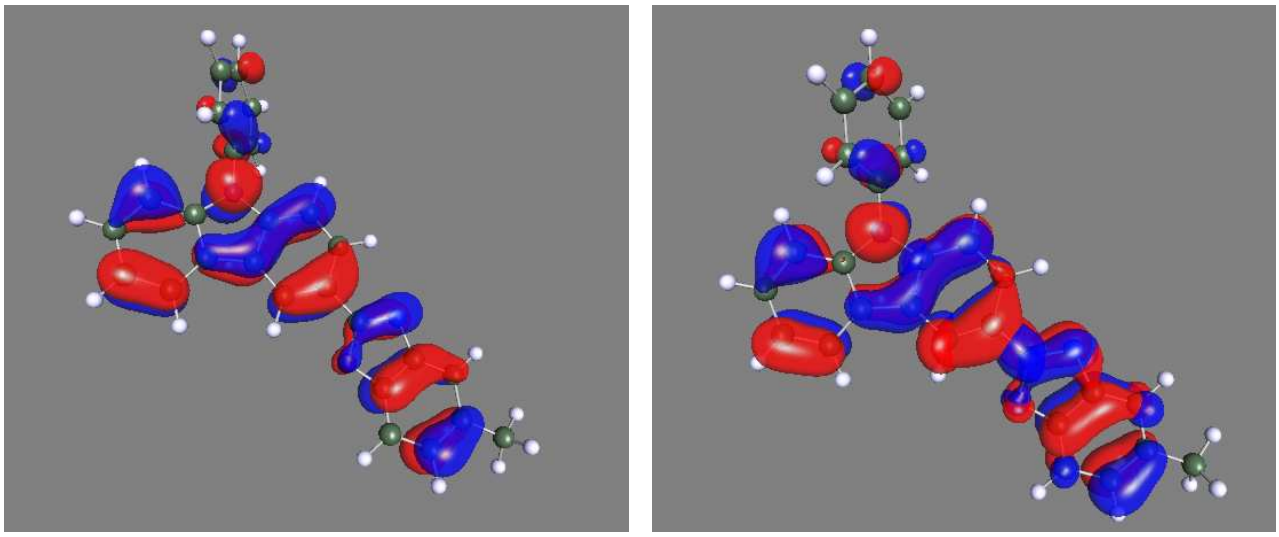

Figure 4S. HOMO and LUMO orbitals of **2**.

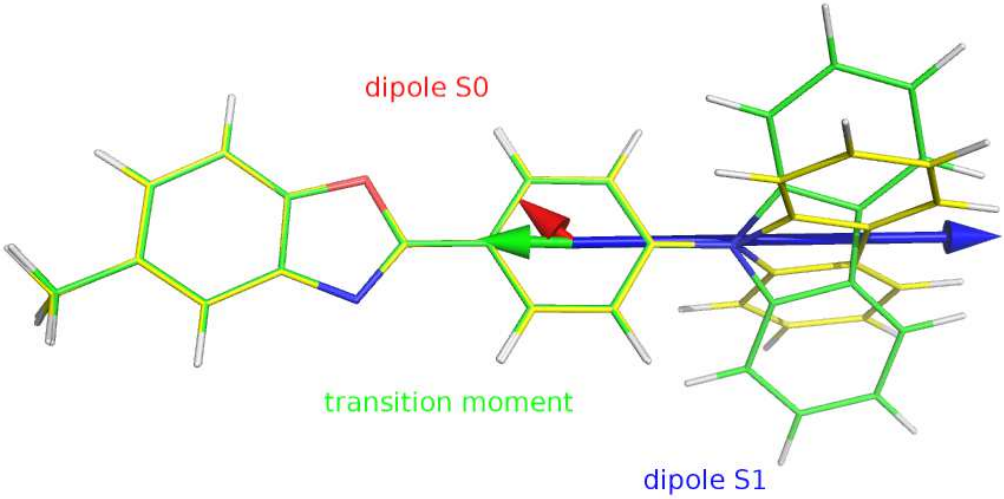

Figure 5S. Theoretically calculated structure of **1** in the ground (green) and excited state (yellow) with the orientation of the dipole moments in the ground (red arrow) and excited state (blue arrow) as well as transition dipole moment in emission (green arrow). The excited state dipole moment and transition dipole moment are enlarged for 3 and 200 times, respectively. The transition dipole moment in absorption is not presented because of overlapping with the transition dipole moment in emission.

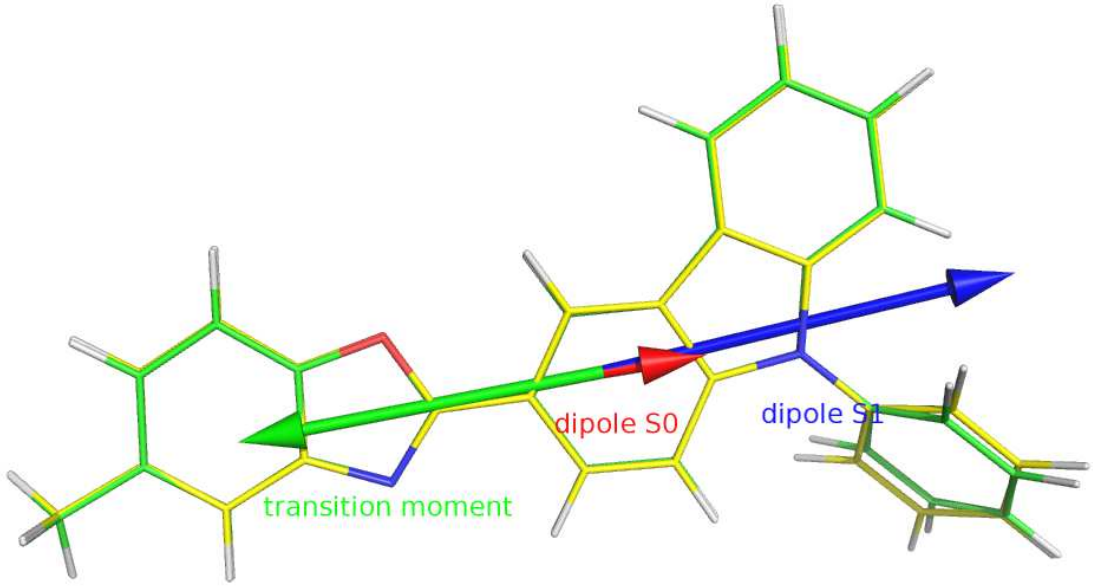

Figure 6S. Theoretically calculated structure of **2** in the ground (green) and excited state (yellow) with the orientation of the dipole moments in the ground (red arrow) and excited state (blue arrow) as well as transition dipole moment in emission (green arrow). The transition dipole moment in absorption is not presented because of too small angle (4.1 degree) between both transition dipole moments.

The experimentally obtained emission anisotropy course can be fitted with the expression obtained by Kawski and Gryczyński:

$$r(\beta, R_d) = r(R_d)\left(\frac{3}{2}\cos^2\beta - \frac{1}{2}\right)$$

$$r(R_d) = \frac{3}{2}\frac{\left(a^2-1\right)+2a^2\left(a^2-1\right)^{-\frac{1}{2}}-3a^2\arcsin\left(\frac{1}{a}\right)}{2\left(a^2-1\right)^{-\frac{1}{2}}-2\arcsin\left(\frac{1}{a}\right)}-\frac{1}{2}$$

where: $a^2 = \frac{R_d^2}{\left(R_d^2-1\right)}$

R_d denotes the stretching factor and β denotes the angle between the transition dipole moment in absorption and emission.

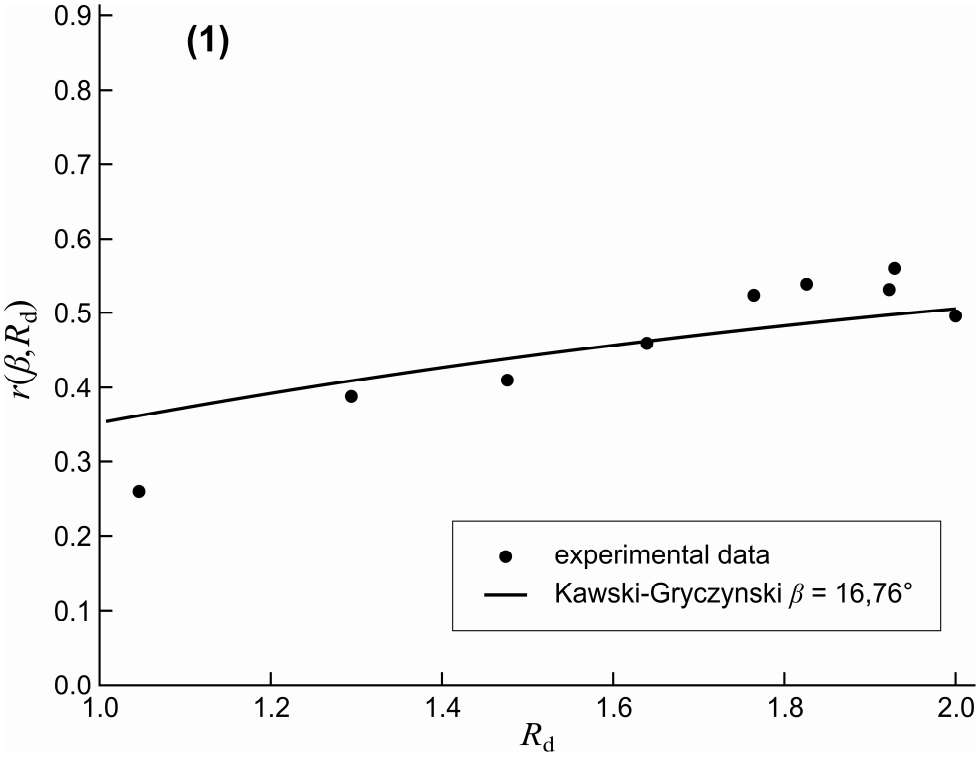

Figure 7S. Emission anisotropy versus linear dichroism R_d for **1** in PVA film at 293 K. Solid line has been obtained from Kawski-Gryczyński model and the best fit to experimental data was obtained for the value of β specified in the text box.

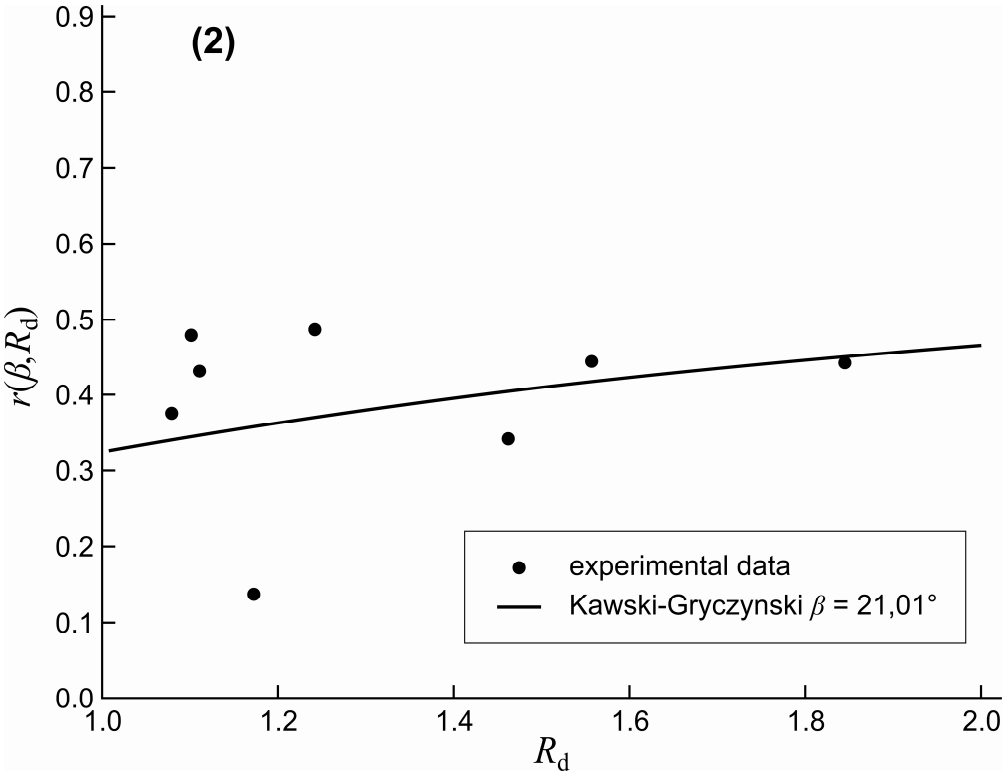

Figure 8S. Emission anisotropy versus linear dichroism R_d for **2** in PVA film at 293 K. Solid line has been obtained from Kawski-Gryczynski model and the best fit to experimental data was obtained for the value of β specified in the text box.